crystals

MDPI

Article

Potential Role of 'Green' Synthesized Titanium Dioxide Nanoparticles in Photocatalytic Applications

Manal A. Awad [1,*], Meznah M. Alanazi [2,*], Awatif A. Hendi [2], Promy Virk [3], Albandari W. Alrowaily [2], Taghreed Bahlool [2], Fatehia S. Alhakami [4], Fatma Aouaini [2] and Eiman Mamoun Ibrahim [5]

1 King Abdullah Institute for Nanotechnology, King Saud University, Riyadh 11451, Saudi Arabia
2 Department of Physics, College of Science, Princess Nourah bint Abdulrahman University, Riyadh, Saudi Arabia
3 Department of Zoology, King Saud University, Riyadh 11451, Saudi Arabia
4 Faculty of Science and Humanity, Hotat Bani Tamim, Prince Sattam Bin Abdulaziz University, Al-Kharj 16278, Saudi Arabia
5 Central Lab & Prince Naif Centre for Heath Science Research, King Saud University, Riyadh 11459, Saudi Arabia
* Correspondence: mawad@ksu.edu.sa (M.A.A.); mmalenazy@pnu.edu.sa (M.M.A.)

Abstract: Environmental sustainability is the cornerstone of the development of nanotechnology in today's time. The synthesis of nanoparticles (NPs) based on green chemistry widely promotes this concept by minimizing the use of toxic precursors. Herein, the synthesis of titanium dioxide (TiO_2) NPs is reported using *Origanum majorana* extract. The mode of synthesis is facile, eco-friendly, economically, applicable, and rapid. The constituent phytochemicals of the extract responsible for the formation of the nanocatalysts were identified using FTIR spectroscopy. In addition, X-ray diffraction, particle size measurements, and transmission electron microscopy were used to characterize the nanocatalysts. Moreover, the ability of TiO_2 NPs to degrade rhodamine B dye under UV irradiation was also investigated. The key findings showed the marked photocatalytic property of the synthesized green TiO_2 NPs, which could be potentially incorporated as a nanoscale technique in the process of water purification for human use.

Keywords: titanium dioxide; *Origanum majorana*; rhodamine B dye; catalytic degradation

Citation: Awad, M.A.; Alanazi, M.M.; Hendi, A.A.; Virk, P.; Alrowaily, A.W.; Bahlool, T.; Alhakami, F.S.; Aouaini, F.; Ibrahim, E.M. Potential Role of 'Green' Synthesized Titanium Dioxide Nanoparticles in Photocatalytic Applications. *Crystals* **2022**, *12*, 1639. https://doi.org/10.3390/cryst12111639

Academic Editors: Assem Barakat, Ayman El-Faham, Saied Soliman and Ingo Dierking

Received: 20 October 2022
Accepted: 9 November 2022
Published: 14 November 2022

1. Introduction

Nanoparticles (NPs) are distinguished from the particles of bulk material based on NPs large surface area to volume ratio [1]. In recent years, the literature has been replete with the extensive use of transition-metal-oxide semiconductors. Titanium dioxide (TiO_2) is a commonly used semiconductor in a range of industrial and consumer products in addition to the photodegradative clearing of organic contaminants in the atmosphere and water [2]. Photocatalysis has vast potential for environmental applications [3].

TiO_2 is one of the most promising and popular metal oxides used in photocatalysis. It is widespread photocatalytic applications that attributed to its potent oxidizing ability, high photostability, and redox activity [4,5]. It is also important among the n-type semiconductors, owing to its properties: photoabsorption, surface desorption, and transport of charge properties [6]. TiO_2 exists in three crystalline structures, namely anatase, rutile, and brookite, out of which the anatase phase has the widest applications, including being used in photovoltaic cells [7], in photocatalysis, and as an antimicrobial agent [8]. The absorption of photons energy by TiO_2 at a rate equal to or more than its band gap (~3.2 eV) promotes the transfer of valence electrons to the conduction band, thus creating voids in the valence band. These photogenerated electrons and voids trigger redox reactions in the molecules adsorbed on the surface of TiO_2. Thus, TiO_2 is used as a semiconductor primarily is due to its ability to cause photon-induced electron transfer [9,10].

Herein, TiO_2 NPs were synthesized using *Origanum majorana* (*Mardagoosh*) extract via green chemistry [11]. In comparison to conventional modes, the mode applied in this study is prudent, facile, and based on the potent ability of TiO_2 NPs to photodegrade rhodamine B (Rh B) dye. The photodegradation of Rh B was confirmed by assessing the photocatalytic activity of green TiO_2 NPs irradiated with visible light.

2. Materials and Methods

2.1. Synthesis of TiO_2 Nanoparticles

After washing, drying, and grinding the fresh herb, *Origanum majorana*, 10 g was added to 100 mL of boiled distilled water. This was followed by filtration of the extract, and the combined filtrates were used to prepare the NPs.

Titanium (IV) isopropoxide (TTIP) and herb extract were mixed in a ratio of volume 1:2 under constant stirring for 2 h at room temperature until a yellowish solution appeared. Thereafter, heating the solution at 80 °C on a hot plate for an hour produced a paste. This paste was then reduced to powder form and calcined (dried) in a muffle furnace at 450 °C for 5 h. The resulting beige powder contained TiO_2 NPs.

2.2. Characterization of Green TiO_2 Nanoparticles

The characterization included powder XRD, with the diffraction angle range (2θ) set between 20° and 90°, using Bruker D8 ADVANCE (Bruker, Billerica, MA, USA) operating at 40 KV and 40 MA with CuKa radiation at 1.5418 Å. Transmission electron microscopy (TEM) (JEM-1400, JEOL, Tokyo, Japan) was used to determine the morphology and distribution of the NPs. Energy-dispersive spectroscopy (EDS, JSM-7610F, JEOL, Peabody, MA, USA) was carried out using a scanning electron microscope equipped with an EDX attachment (JSM-6390 172, JEOL, Tokyo, Japan) to determine the elemental map of the particles. Fourier transform infrared (FTIR) spectra in the range of 400–4000 cm^{-1} were recorded using a Perkin-Elmer 100 spectrophotometer. The stability and particle size distribution of the NPs were measured with a dynamic light scattering technique (DLS) using a Zetasizer (HT Laser, ZEN3600 Malvern, Cambridge, UK). The optical properties of the synthesized TiO_2 NPs and the dye degradation were recorded by the absorbance spectra of the samples (supernatants) using a UV-1800 UV-Vis spectrometer (Shimadzu, Riverwood Dr, Columbia, MD, USA) in the range of 200–1100 nm.

2.3. Photocatalytic Measurement

The photocatalytic activity of the NPs was assessed under ultraviolet irradiation lamp with Rh B dye. For this, a laboratory-scale cuvette was filled with 6×10^{-6} M of dye solution, and the photocatalyst sample was dispersed inside the cuvette under exposure to UV light at a distance of 5 cm from the lamp (365 nm: 0.7 AMPS) and was continuously stirred during the degradation test. At varied durations of light exposure, the recorded optical absorption spectra assessed the rate of degradation on the basis of a lowering in the intensity of absorption by the dye at the maximum wavelength (λmax = 553 nm). The degradation efficiency (DE) was evaluated based on the following formula:

$$DE\% = (A_0 - A)/A_0 \times 100$$

where A_0 is the initial absorption intensity of wastewater at λ_{max} = 553 nm, and A is the absorption intensity after photodegradation.

3. Results and Discussion

3.1. X-ray Diffraction Analysis of Titanium Dioxide

XRD patterns of the green-synthesized TiO_2 NPs are shown in Figure 1. The diffraction peaks and crystallographic planes of the synthesized TiO_2 NPs are located at 2θ values of 27.540° (1 0 1), 36.182° (1 0 3), 38.660° (0 0 4), 44.146° (2 0 0), 54.382° (1 0 5), 56.758° (2 1 1),

62.835° (2 0 4), 64.5° (213), 68.968° (1 1 6) and 70.418° (2 2 0), respectively (COD 9009086), thus confirming the formation of TiO_2 NPs in the anatase phase.

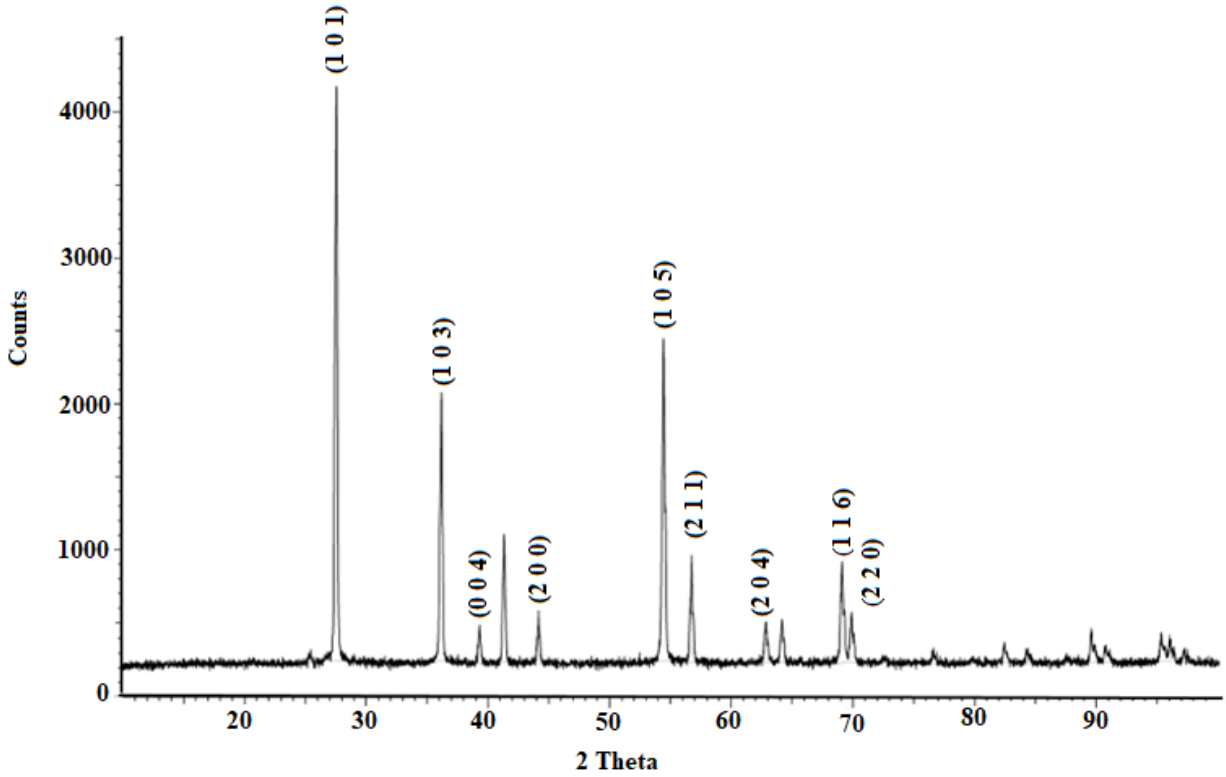

Figure 1. X-ray diffraction patterns of green TiO_2 nanoparticles.

The Scherrer formula, $D = 0.9\lambda/\beta \cos\theta$, was used to evaluate the mean size of the synthesized NPs, where λ is the X-ray wavelength (equal to 0.15409 nm), β represents the full width at half maximum (FWHM) of the diffraction peak, θ denotes the Bragg diffraction angle, and D denotes the crystallite size. Based on these calculations, an average crystallite size of the NPs was observed to be 42.1 nm. The presence of sharp peaks validated the anatase form, while the absence of peaks represented other crystallite forms of TiO_2 [12,13].

3.2. Particle Size Measurements

As illustrated in Figure 2, the particles are semi-monodispersed, with a 0.312 polydispersity index (PDI), and have an average size of the approximately 238 nm as measured using the DLS technique.

3.3. Transmission Electron Microscopic Analysis

The size, shape, crystallinity, and morphology of the green TiO_2 NPs were evaluated using TEM. Figure 3 shows that all of the NPs are monodispersed with a certain degree of agglomeration, which corroborates the DLS intensity distribution results. The NPs were observed to be irregular (Figure 3a) and hexagonal (Figure 3b) in shape and moderately variable in size. The micrographs clearly depict the distribution and dispersion with the extent of the exfoliation, intercalation, and orientation of the NPs. The crystallographic structures of the samples are clearly reflected in the images [14]. The TiO_2 NPs reflect good crystallinity being in the anatase phase, with dotted concentric rings that contribute to the irregular shape of TiO_2, which was also observed in the XRD patterns [15].

		Size (d.nm):	% Intensity:	St Dev (d.nm):
Z-Average (d.nm): 238.0	Peak 1:	186.2	100.0	75.59
PdI: 0.312	Peak 2:	0.000	0.0	0.000
Intercept: 0.783	Peak 3:	0.000	0.0	0.000

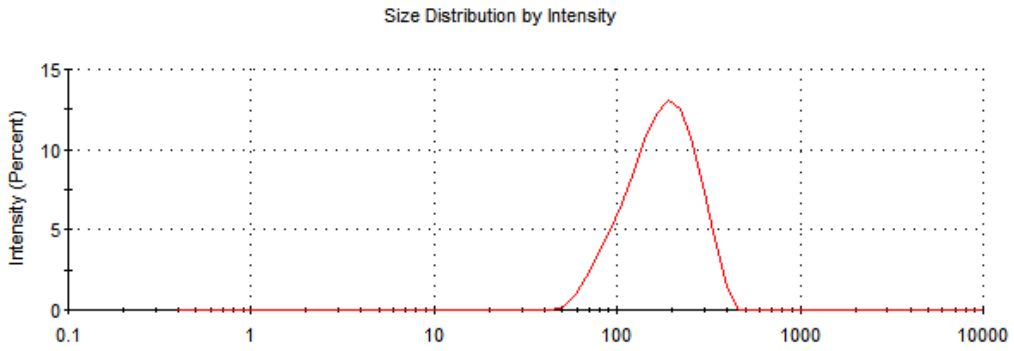

Figure 2. Z- Average and Size distribution of green TiO_2 nanoparticles.

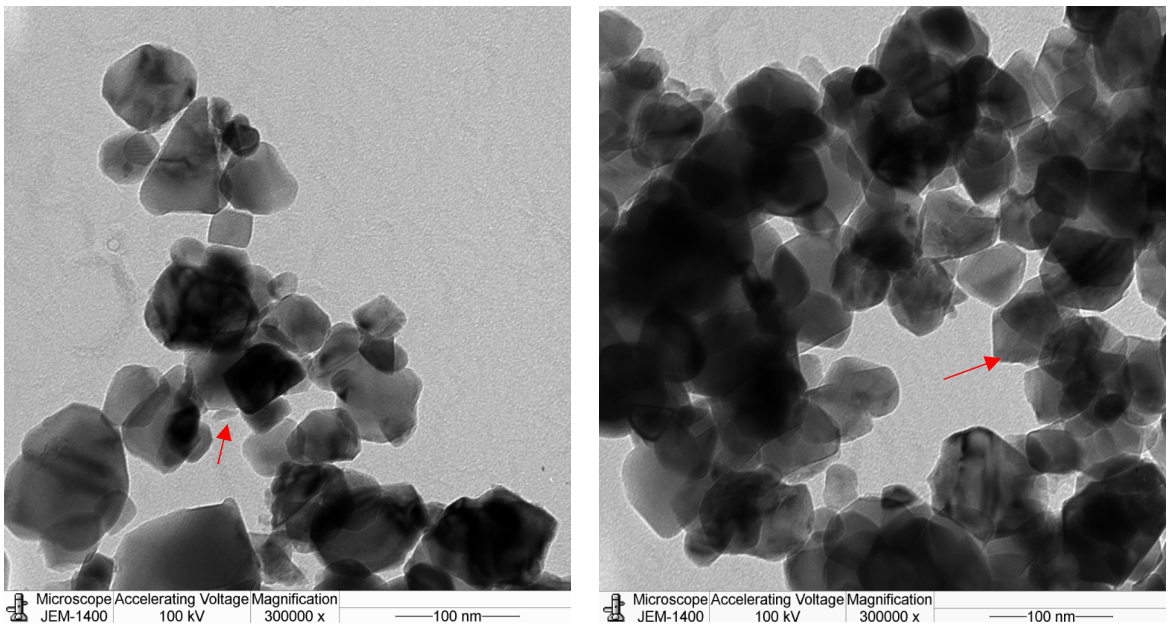

(**a**) (**b**)

Figure 3. Transmission electron microscopy images of green TiO_2 nanoparticles. (**a**) irregular (**b**) hexagonal in shape.

3.4. Energy-Dispersive Spectroscopy Analysis

EDS analysis validated the crystalline nature of the metallic TiO_2 NPs. Figure 4 indicates that oxygen and titanium elements were detected; the presence of other peaks reflects the surface adsorption of extracellular organic moieties on the NPs.

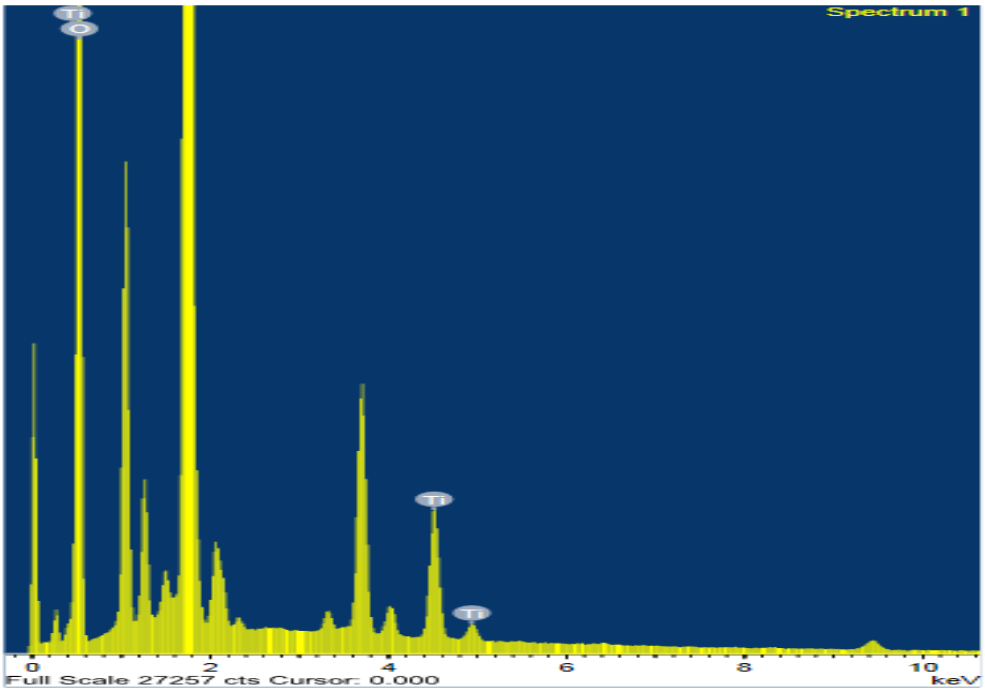

Figure 4. Energy-dispersive spectroscopy results showing the chemical composition of the green TiO_2 nanoparticles.

3.5. Fourier Transform Infrared Analysis

FTIR spectra of the TiO_2 NPs are illustrated in Figure 5. The spectrum of $TiO(OH)_2$ shows characteristic bands at 3422.75 cm^{-1} and 1622.03 cm^{-1} corresponding to the surface water or hydroxyl groups and carbonyl groups, respectively. The peak at 1622.03 cm^{-1} corresponds to the O–H bending vibrations due to the adsorbed water molecules on the surface of TiO_2, which play a vital role in the photocatalysis. The peaks in the broad band centered at 461.12 cm^{-1} correspond to the reduction of TiO_2 by *Murdagoosh*, and this distinctive bending mode of vibration of the Ti–O corroborates the bond between the oxygen and metal [16,17]. The broad peak demonstrated at 3389 cm^{-1} corresponds to stretching vibrations of –O–H [18,19]. Furthermore, no other peaks related to the organic moiety were observed.

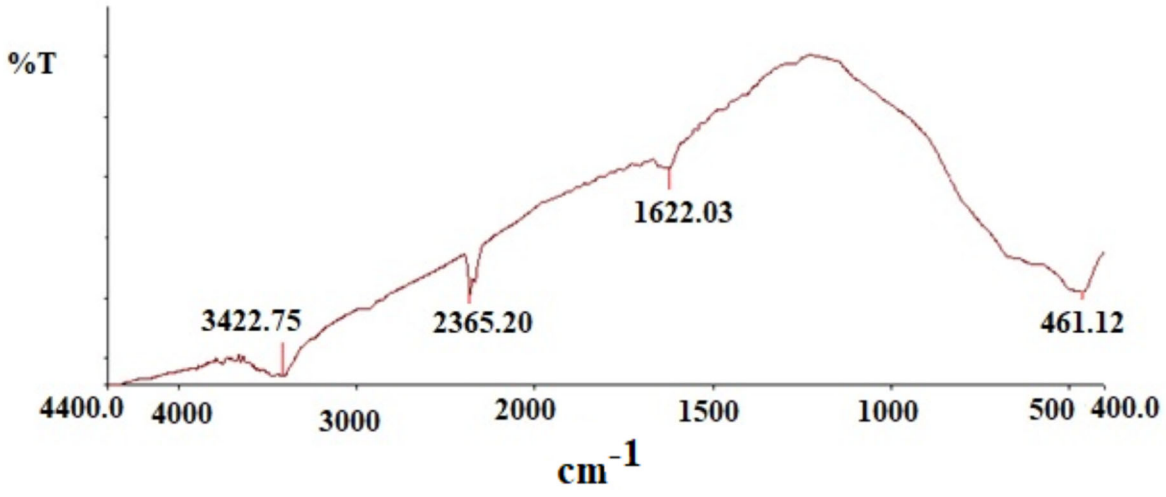

Figure 5. Fourier-transform infrared spectra of TiO_2 nanoparticles with aqueous extract of Murdagoosh.

3.6. Photocatalytic Activity of Green TiO_2

The degradation of Rh B via photocatalysis in an aqueous medium at an ambient temperature under UV-vis irradiation assessed the photocatalytic activity of the TiO_2 NPs. A temporal quantification was recorded every 10 h post exposure to UV light for the dye mixed with the photocatalyst. A reduction in the intensity of the peak was observed after exposure of the treated dye to UV light. The decrease in UV absorbance mirrors a reduction in the concentration of Rh B, which was detectable as the decrease in the intensity of the pink color of Rh B dye that changed gradually to a colorless solution [20,21]. As shown in Figure 6, the green TiO_2 catalyst responded well under UV irradiation, with 100% removal after 20 h of irradiation. These observed changes are ascribed to the absorption of photons with an enhanced number of active sites on the catalyst.

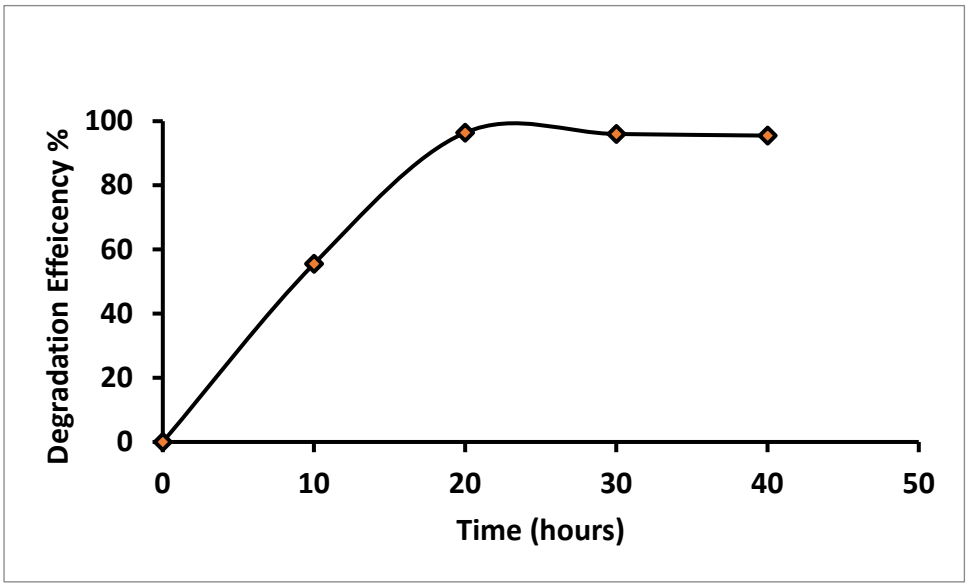

Figure 6. Degradation efficiency of green TiO_2 under UV irradiation.

3.7. Degradation Mechanism

It has been postulated that, following UV irradiation the valence electrons of TiO_2 become excited; cross the valence band, and move to the conduction band, creating holes in the valence band, as illustrated in Figure 7.

This is best explained by the fact that after absorption of energy rich photons higher than the band gap energy (Eg), electrons (e^-) in a catalyst are excited and moved from the valence band to the conduction band, leaving behind an electron void or hole (h^+) in the valence band, as shown in Equation (1).

$$TiO_2NPs + h\nu(\text{Photon Energy}) \rightarrow \text{Electron}_{cb}\ (e^-) + h_{vb}{}^+ \rightarrow (\text{Electron-hole generation}) \quad (1)$$

These generated e^- and h^+ pairs can move to the catalyst surface where they react with the surface hydroxyl groups (OH•) or water and dissolved oxygen to form hydroxyl, peroxide (H_2O_2.), and superoxide radical anions (O_2•−), as shown in Equations (2)–(6).

$$TiO_2NPs\ (h_{vb}{}^+) + (H_2O)_{\text{absorbed}} \rightarrow H^+ + TiO_2NPs + {}^{\bullet}OH \quad (2)$$

$$TiO_2NPs(h_{vb}{}^+) + \text{Organic}\ (OH^-) \rightarrow TiO_2NPs + \text{Oxidation products}\ (\bullet OH) \quad (3)$$

$$TiO_2NPs(e^-{}_{cb}) + \text{Oxygen}(O_2) \rightarrow TiO_2NPs + O2\bullet^- \quad (4)$$

$$O_2\bullet^- + H^+ \rightarrow \text{Hydroperoxyl radical}\ (HO_2\bullet) \quad (5)$$

$$O_2\ \text{ions} TiO_2NPs\ (e_{cb}{}^-) + \text{Organic}\ (H_2O_2) \rightarrow + TiO_2NPs + \text{Reduction products}\ (\bullet OH + OH^-) \quad (6)$$

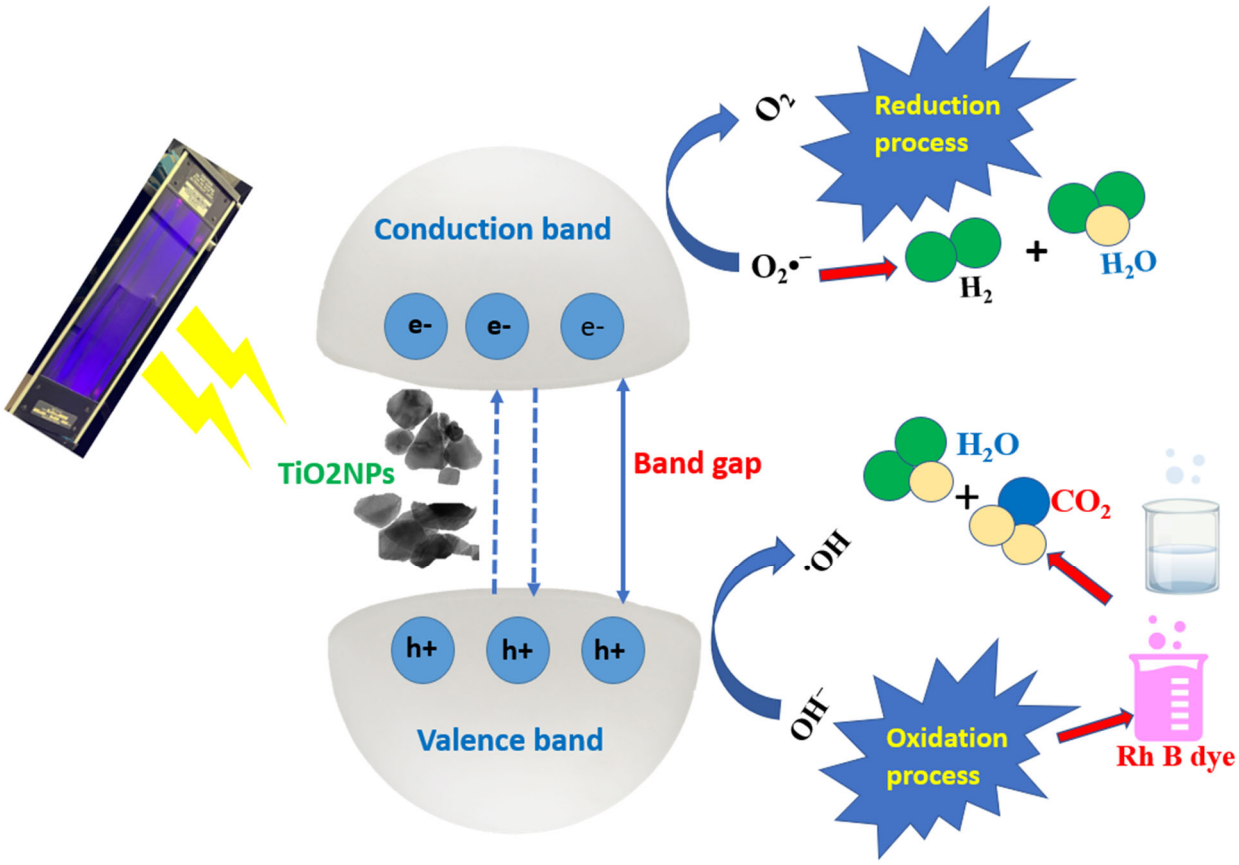

Figure 7. Illustration of the mechanism of photocatalysis, proving degradation of Rh B pollutant dye using synthesized TiO_2 NPs as photocatalysts.

The engendered holes/voids react with the oxygen ions on the surface to form •OH radicals, as shown in Equation (7). These engendered radicals subsequently react with the dye to generate a gamut of intermediates, which include radicals and radical cations; moreover, the formation of carbon dioxide, dihydrogen monoxide, and inorganic nitrogen with nitrate ions ensues, resulting in complete mineralization.

$$\text{RhB dye} + \bullet\text{OH} \rightarrow \text{oxidized products} \rightarrow \text{degradation products } (CO_2 + H_2O + NO_3^- + NH_4^+) \quad (7)$$

The oxidized products formed are thus mineralized into CO_2, H_2O, NO_3^-, and NH_4^+ [22,23].

The photogenerated holes possess a potent ability to capture the electrons of the Rh B onto the TiO_2 surface. Subsequently, active oxidation of Rh B occurs, resulting in the photodegradation of the dye. When exposed to UV light, the generation of electrons by the green TiO_2 NPs increases. The increased surface area decreases the density of electron accumulation on the surface. TiO_2 can interact fully with organic matter owing to the wide surface area of the particles, which also improves the adsorption of more organic matter on the surface. As a result, an integrated process from adsorption to reaction is ensured by the adsorptive capacity. The photocatalytic reaction system then separates the reacting chemicals, which ultimately results in an increase in photocatalytic efficiency [24,25]. Oxygen easily obtains photogenerated electrons from the surface of the green TiO_2 NPs to form $O_2\bullet^-$ [26,27]. The TiO_2 NPs possess a larger surface area to absorb more oxygen; hence, they have a potent oxidant status to effectively degrade the dye. This contributes to the greater photocatalytic efficacy of the NPs. The outstanding photodegradation of the synthesized NPs highlights their potential applications under UV or direct solar irradiation in water treatment plants [28].

In comparison of our findings with other outcomes of similar research that using different plants extracts, chemical methods to synthesize TiO NPs or composite/TiO NPs, it has been found that, *origanum majorana* extract synthesize TiO_2 NPs occupies an important position due to the higher degradation percentage than the others reported as shown in Table 1.

Table 1. Comparative account of published data showing performance of different photocatalysts.

TiO_2 NPs Synthesized by	Size of TiO_2 NPs	Source of Photons	Name of Pollutant	Degradation Percentage %
Cochlospermum gossypium gum extract [29]	8–13 nm (TEM)	Sunlight	Methylene blue	Time and pH dependent about 90–100
Phyllanthus Emblica (amla) leaves extract [30]	20–30 nm (TEM)	Solar	Coralline red	93
Sol-gel method [31]	73.99 nm (TEM)	Visible	Methylene blue and methyl orange	73 and 69, respectively
Calotropis gigantea leaf extract [32]	42 nm (TEM)	Visible	Metformin	97
Pullulan extract [33]	28–127 nm (TEM)	UV	Methyl orange and rhodamine B	99 for both dyes
Films grown by metalorganic chemical vapor deposition (MOCVD) method [34]	Thickness of film 468 nm	UV Irradiation	Methyl orange	69
Origanum majorana extract (our study)	238 nm (DLS)	UV Irradiation	Rhodamine B	100

4. Conclusions

The current study accounts for the use of an herbal extract of *Origanum majorana* (*Murdagoosh*) to synthesize TiO_2 NPs. This green reduction of metal oxides is facile, cost-effective, nontoxic, and eco-friendly when forming metal oxide NPs. The key findings showed that the NPs have marked photocatalytic activity, with 100% removal post 20 h of UV irradiation. This technique promises a prospectively safe and affordable nanofiltration technique for obtaining clean, potable water.

Author Contributions: Conceptualization, M.A.A., M.M.A. and A.A.H.; methodology, M.A.A., F.S.A., F.A., E.M.I., A.W.A. and T.B.; validation; formal analysis; and investigation, M.A.A. and P.V.; resources, M.M.A. and A.A.H.; data curation, M.M.A., A.A.H. and P.V.; writing—original draft preparation, M.A.A., M.M.A., A.A.H. and P.V.; writing—review and editing, M.A.A. and P.V.; supervision; project administration, M.A.A., M.M.A. and A.A.H.; funding acquisition, M.M.A. and A.A.H. All authors have read and agreed to the published version of the manuscript.

Funding: This work was funded by the Deanship of Scientific Research at Princess Nourah bint Abdulrahman University, through the Research Groups Program Grant no. (RGP-1443 -0047).

Conflicts of Interest: The authors declare no conflict of interest.

References

1. Irshad, M.A.; Nawaz, R.; Rehman, M.Z.U.; Adrees, M.; Rizwan, M.; Ali, S.; Ahmad, S.; Tasleem, S. Synthesis, characterization and advanced sustainable applications of titanium dioxide nanoparticles: A review. *Ecotoxicol. Environ. Saf.* **2021**, *212*, 111978. [CrossRef] [PubMed]
2. Chand, K.; Cao, D.; Fouad, D.E.; Shah, A.H.; Lakhan, M.N.; Dayo, A.Q.; Sagar, H.J.; Zhu, K.; Mohamed, A.M.A. Photocatalytic and antimicrobial activity of biosynthesized silver and titanium dioxide nanoparticles: A comparative study. *J. Mol. Liq.* **2020**, *316*, 113821. [CrossRef]
3. Reddy, N.L.; Rao, V.N.; Kumari, M.M.; Kakarla, R.R.; Ravi, P.; Sathish, M.; Karthik, M.; Venkatakrishnan, S.M. Inamuddin Nanostructured semiconducting materials for efficient hydrogen generation. *Environ. Chem. Lett.* **2018**, *16*, 765–796. [CrossRef]
4. Rahimi, N.; Pax, R.A.; Gray, E.M. Review of functional titanium oxides. I: TiO_2 and its modifications. *Prog. Solid State Chem.* **2016**, *44*, 86–105. [CrossRef]
5. Ilhan, H. A Comparative Study on the Photocatalytic Activity of Dye-Sensitized and Non-Sensitized Graphene Oxide-TiO_2 Composites under Simulated and Direct Sunlight. Master's Thesis, Izmir Institute of Technology, Izmir, Turkey, 2019.

6. Syetali, M.; Anuratha, V.; Akila, M.; Yogananth, N. Anti genotic effect of TiO_2 nanoparticles biosynthesized from sargassum polycystum- a marine macroalage. *J. Nanomed. Res.* **2017**, *5*, 25.
7. Kiwaan, H.; Atwee, T.; Azab, E.; El-Bindary, A. Photocatalytic degradation of organic dyes in the presence of nanostructured titanium dioxide. *J. Mol. Struct.* **2019**, *1200*, 127115. [CrossRef]
8. Su, C.; Hong, B.-Y.; Tseng, C.-M. Sol–gel preparation and photocatalysis of titanium dioxide. *Catal. Today* **2004**, *96*, 119–126. [CrossRef]
9. Chen, H.-S.; Su, C.; Chen, J.-L.; Yang, T.-Y.; Hsu, N.-M.; Li, W.-R. Preparation and Characterization of Pure Rutile TiO_2 Nanoparticles for Photocatalytic Study and Thin Films for Dye-Sensitized Solar Cells. *J. Nanomater.* **2011**, *2010*, 869618. [CrossRef]
10. Yao, S.; Tang, H.; Liu, M.; Chen, L.; Jing, M.; Shen, X.; Li, T.; Tan, J. TiO_2 nanoparticles incorporation in carbon nanofiber as a multi-functional interlayer toward ultralong cycle-life lithium-sulfur batteries. *J. Alloys Compd.* **2019**, *788*, 639–648. [CrossRef]
11. Awad, M.A.; Hend, A.A.; Ortashi, K.M.O.; Alenazi, W. Synthesis of Titanium Dioxide Nanoparticles Using Origanum Majorana Herbal Extracts. U.S. Patent 10,138,135 B1, 27 November 2018.
12. Kandiel, T.A.; Robben, L.; Alkaima, A.; Bahnemann, D. Brookite versus anatase TiO_2 photocatalysts: Phase transformations and photocatalytic activities. *Photochem. Photobiol. Sci.* **2013**, *12*, 602–609. [CrossRef]
13. Shanavas, S.; Priyadharsan, A.; Karthikeyan, S.; Dharmaboopathi, K.; Ragavan, I.; Vidya, C.; Acevedo, R.; Anbarasana, P. Green synthesis of titanium dioxide nanoparticles using Phyllanthus niruri leaf extract and study on its structural, optical and morphological properties. *Mater. Today Proc.* **2020**, *26*, 3531–3534. [CrossRef]
14. Tarafdar, A.; Raliya, R.; Wang, W.-N.; Biswas, P.; Tarafdar, J.C. Green Synthesis of TiO_2 Nanoparticle Using Aspergillus tubingensis. *Adv. Sci. Eng. Med.* **2013**, *5*, 943–949. [CrossRef]
15. Hariharan, D.; Srinivasar, K.; Nehru, L.C. Synthesis and characterization of TiO_2 nanoparticles using Cynodon Dactylon leaf extract for antibacterial and anticancer (A549 Cell Lines) activity. *J. Nanomed. Res.* **2017**, *5*, 00138.
16. Khade, G.V.; Suwarnkar, M.B.; Gavade, N.L.; Garadkar, K.M. Green synthesis of TiO_2 and its photocatalytic activity. *J. Mater. Sci. Mater. Electron.* **2015**, *26*, 3309–3315. [CrossRef]
17. Gao, Y.; Masuda, Y.; Peng, Z.; Yonazawa, T.; Kaumoto, K. Room temperature deposition of a TiO_2 thin film from aqueous peroxotitanate solution. *J. Mat. Chem.* **2007**, *13*, 608. [CrossRef]
18. Gomes, J.; Lincho, J.; Domingues, E.; Quinta-Ferreira, R.M.; Martins, R.C. N–TiO_2 Photocatalysts: A Review of Their Characteristics and Capacity for Emerging Contaminants Removal. *Water* **2019**, *11*, 373. [CrossRef]
19. Maślana, K.; Żywicka, A.; Wenelska, K.; Mijowska, E. Boosting of Antibacterial Performance of Cellulose Based Paper sheet via TiO_2 Nanoparticles. *Int. J. Mol. Sci.* **2021**, *22*, 1451. [CrossRef]
20. Kunze, J.; Ghicov, A.; Hildebrand, H.; Macok, J.M.; Traveira, L.; Schmuki, P. Challenges in the Surface Analytical Characterisation of Anodic TiO_2 Films—A Review. *Phys. Chem.* **2005**, *219*, 1561.
21. Kothavale, V.P.; Patil, T.S.; Patil, P.B.; Bhosale, C.H. Photoelectrocatalytic degradation of Rhodamine B using N doped TiO2 thin Films. *Mater. Today: Proc.* **2020**, *23*, 382–388. [CrossRef]
22. Darus, T.M.M.; Muktar, J. Degradation of Rhodamine B Dye by TiO_2 Nanotubes Photocatalyst Synthesized via Alkaline Hydrothermal Method. MATEC Web of Conferences, 27, 03004. 2015. Available online: http://www.matec-conferences.org (accessed on 20 October 2015).
23. Goyal, R.; Kishore, D. Investigation of photocatalytic degradation of rhodamine B by using nano-sized TiO_2. *Int. J. Sci. Res. Manag.* **2017**, *5*, 6006–6013.
24. Ahmed, M.A.; Abou-Gamra, Z.M.; Medien, H.A.A.; Hamza, M.A. Effect of porphyrin on photocatalytic activity of TiO_2 nanoparticles toward rhodamine B photodegradation. *J. Photochem. Photobiol. B* **2017**, *176*, 25–35. [CrossRef] [PubMed]
25. Wang, S.; Shi, X.; Shao, G.; Duan, X.; Yang, H.; Wang, T. Preparation, characterization and photocatalytic activity of multi-walled carbon nanotube-supported tungsten trioxide composites. *J. Phys. Chem. Solids* **2008**, *69*, 2396–2400. [CrossRef]
26. Dash, L.; Biswas, R.; Ghosh, R.; Kaur, V.; Banerjee, B.; Sen, T.; Patil, R.A.; Ma, Y.-R.; Haldar, K.K. Fabrication of mesoporous titanium dioxide using azadirachta indica leaves extract towards visible-light-driven photocatalytic dye degradation. *J. Photochem. Photobiol. A Chem.* **2020**, *400*, 112682. [CrossRef]
27. Oh, Y.-C.; Bao, Y.; Jenks, W.S. Isotope studies of photocatalysis: TiO_2-mediated degradation of dimethyl phenylphosphonate. *J. Photochem. Photobiol. A Chem.* **2003**, *161*, 69–77. [CrossRef]
28. Sonker, R.K.; Hitkari, G.; Sabhajeet, S.; Sikarwar, S.; Rahul; Singh, S. Green synthesis of TiO_2 nanosheet by chemical method for the removal of Rhodamin B from industrial waste. *Mater. Sci. Eng. B* **2020**, *258*, 114577. [CrossRef]
29. Saranya, K.S.; Padil, V.V.T.; Senan, C.; Pilankatta, R.; Saranya, K.; George, B.; Wacławek, S.; Černík, M. Green Synthesis of High Temperature Stable Anatase Titanium Dioxide Nanoparticles Using Gum Kondagogu: Characterization and Solar Driven Photocatalytic Degradation of Organic Dye. *Nanomaterials* **2018**, *8*, 1002. [CrossRef] [PubMed]
30. Singh, A.; Goyal, V.; Singh, J.; Rawat, M. Structural, morphological, optical and photocatalytic properties of green synthesized TiO_2 NPs. *Curr. Res. Green Sustain. Chem.* **2020**, *3*, 100033. [CrossRef]
31. Haque, F.Z.; Nandanwar, R.; Singh, P. Evaluating photodegradation properties of anatase and rutile TiO_2 nano-particles for organic compounds. *Optik* **2017**, *128*, 191–200. [CrossRef]
32. Prashanth, V.; Priyanka, K.; Remya, N. Solar photocatalytic degradation of metformin by TiO_2 synthesized using *Calotropis gigantea* leaf extract. *Water Sci. Technol.* **2021**, *83*, 1072–1084. [CrossRef]

33. Isa, E.D.M.; Shameli, K.; Jusoh, N.W.C.; Hazan, R. Rapid photodecolorization of methyl orange and rhodamine B using zinc oxide nanoparticles mediated by pullulan at different calcination conditions. *J. Nanostructure Chem.* **2020**, *11*, 187–202. [CrossRef]
34. Yang, D. (Ed.) *Titanium Dioxide: Material for a Sustainable Environment*; IntechOpen: London, UK, 2018.